

## RESEARCH ARTICLE

# Mammalian Mediator 19 Mediates H1299 Lung Adenocarcinoma Cell Clone Conformation, Growth, and Metastasis

Lu-Lu Xu, Shu-Liang Guo\*, Su-Ren Ma, Yong-Ai Luo

### Abstract

Mammalian mediator (MED) is a multi-protein coactivator that has been identified by several research groups. The involvement of the MED complex subunit 19 (MED 19) in the metastasis of lung adenocarcinoma cell line (H1299), which expresses the MED 19 subunit, was here investigated. When MED 19 expression was decreased by RNA interference H1299 cells demonstrated reduced clone formation, arrest in the S phase of the cell cycle, and lowered metastatic capacity. Thus, MED 19 appears to play important roles in the biological behavior of non-small cell lung carcinoma cells. These findings may be important for the development of novel lung carcinoma treatments.

**Keywords:** Mammalian mediator (MED) 19 - RNAi - clone conformation - growth - metastasis

*Asian Pacific J Cancer Prev*, 13, 3695-3700

### Introduction

Mammalian mediator (MED) is a multi-protein coactivator identified in several laboratories. MED is an important RNA polymerase II transcription unit and it plays a critical role in the activation and repression of eukaryotic mRNA synthesis (Kim et al., 1994; Boyer et al., 1999; Conaway et al., 2005). Structural and functional studies have found that MED can be subdivided into four distinct modules: the head, the middle, the tail, and the Cyc-C modules. The first three modules form the core functional MED complex, whereas the Cyc-C module is variably associated with the core (Myers and Kornberg, 2000; Bjorklund and Gustafsson, 2005; Baidoobonso et al., 2007). MED reacts through direct interactions with transcription factors that are bound to enhancers and to upstream promoter elements, as well as with polymerase and the general initiation factors at the core promoter (Gu et al., 1999; Bjorklund and Gustafsson, 2005). Mediator complex subunit 19 (MED 19) was discovered in 2002; it was cloned from two large cell lung cancer cell lines that differed in metastatic potential. MED 19 is also called lung cancer metastasis-related protein 1 (LCMR1). Northern blot analysis confirmed that MED 19 is highly expressed in the human lung cancer 95D cell line, which has a high metastatic potential. However, in lung cancer 95C cells, which have weak metastatic ability, MED 19 is expressed at low levels. Considering MED 19 plays a role in carcinoma cell metastasis, the current study was designed to test its function (Sato et al., 2003; 2004). RNA interference (RNAi) target site was screened on exon 2 of the MED 19 gene and a novel MED 19 RNAi lentivirus (M19-pGCSIL) was constructed. To detect biological

behavioral changes after MED 19 protein silencing, the H1299 cell line transfected with M19-pGCSIL was cultured and observed for cell colony morphology, cell cycle examination, and invasion capability. These data are important for the further exploration of oncology therapies (Wang et al., 2011).

### Materials and Methods

#### Materials

Polymerase chain reaction (PCR) reagents, primers, the vshRNA vector (pGCSIL-GFP), the PSC-NC negative vector, and the H1299 cell line were purchased from the Shanghai GeneChem Co., Ltd. The M-MLV kit was purchased from Promega. The SYBR Master Mix kit was obtained from TaKaRa. The pEGFP-N1-3FLAG vector was obtained from BD Bioscience. The Cell Invasion Assay Kit was obtained from Chemicon International. The restriction enzymes were obtained from New England Biolabs. The mouse anti-FLAG antibodies were obtained from Sigma. The mouse anti-GAPDH and goat anti-mouse IgG antibodies were obtained from Santa Cruz.

#### MED 19 expression vector construction

Upstream and downstream primers were designed and generated according to the full-length human MED 19 (sense: 5'-CCG CTC GAG ATG GAG AAT TTC ACG GCA CTG-3' and antisense: 5'-GGG GTA CCG TAC TGG GTT TAC CTG GGG GGA C-3'). The following components were added to the reaction: 0.4  $\mu$ l of each primer, 2  $\mu$ l of 10 $\times$  buffer, 0.8  $\mu$ l of dNTPs (25 mM), 0.2  $\mu$ l of Pfu polymerase, 1  $\mu$ l of template DNA (10 ng/ $\mu$ l), and 0.5  $\mu$ l of MgCl<sub>2</sub> (total volume of 20  $\mu$ l). The template

**Table 1. Target Site Sequence**

	Target sequence	GC%	Position in CDS
Target 1	GGTGAAGGAGAAGCTAAGT	47.36%	300-318
Target 2	CTTGGAACAAGCCTATAAT	36.84%	264-282
Target 3	CGAATCTGATCACACACTA	42.11%	242-260
Target 4	GCACGAATCTGATCACACA	47.37%	239-257

Note: Targets 1-4 were four different screening sites on MED 19 CDS; The Target Sequence shows the detailed sequences; All four sequences have the proper GC%

**Table 2. Treatments**

N	M	C	K1	K2	K3	K4
A	OE+EM (0.25 mg)	OE+NC (0.25 mg)	OE+K1 (0.25 mg)	OE+K2 (0.25 mg)	OE+K3 (0.25 mg)	OE+K4 (0.25 mg)
B	OE+EM (0.5 mg)	OE+NC (0.5 mg)	OE+K1 (0.5 mg)	OE+K2 (0.5 mg)	OE+K3 (0.5 mg)	OE+K4 (0.5 mg)

OE, M19-pEGFP-N1; EM, pEGFP-N1-3FLAG; NC, empty viral vector plasmid; K1-K4, viral vector plasmid targeting Med 19 sequences

was acquired from a cDNA library and the PCR reaction cycle was 30 s at 94 °C, 30 s at 55 °C, and 1 min at 72 °C for 30 cycles. The product length was 599 base pairs and contained Xho I and Kpn I sites. The pEGFP-N1-3FLAG and PCR product were cleaved with Xho I and Kpn I (37 °C for 1 h). The resulting PCR product and linearized vector were then ligated at 16 °C for 12 h to form a newly combined plasmid that was transfected and amplified in *Escherichia coli*. Finally, a novel eukaryotic vector-expressed MED 19 was constructed and labeled as M19-pEGFP-N1. This construct was subsequently transfected into 293T cells.

#### RNA interference target site screening

MED 19-targeting oligonucleotides were designed and generated from full-length human MED 19 gene. According to the design rules, four different sequences were chosen and separately distributed on MED 19 (Table 1). The packaging cell line was 293T cells that were preliminarily infected with the MED 19 expression vector (M19-pEGFP-N1). The infected 293T cells were divided into different groups to test MED 19 knockdown efficiency. Group N was not transfected with any vector whereas group M was cotransfected with pEGFP-N1-3FLAG as an interference vector. Group C was transfected with empty viral vector plasmid. Groups K1-K4 were transfected with four different viral vector plasmids targeting MED 19 sequences. All groups were divided into two sections according to the concentration of interference vectors, at 0.25 µg and 0.5 µg (Table 2). The interference efficiency was tested by western blot analysis. The primary antibodies used were mouse anti-FLAG (1:5000) and mouse anti-GAPDH (1:5000). The secondary antibody used was goat anti-mouse IgG (1:5000). The test cells were cultured in Dulbecco's modified Eagle's medium.

Group N consisted of empty non-infected 293T cells and it was used as the control group. The other groups were transfected with the MED 19 expression vector (M19-pEGFP-N1) and one of the following interference

vectors: Group M with pEGFP-N1-3FLAG vector, Group C with empty viral vector plasmid as the negative control group, and Groups K1-K4 with different viral vector plasmids. All groups were divided into two dosage groups based on the dosage of the interference vectors; Group A was treated with 0.25 µg and Group B was treated with 0.5 µg.

#### Interference in cells naturally expressing MED 19

K3 viral vector plasmid was found to be the most efficient in silencing MED 19. Hence, interference ds-DNA was synthesized according to the K3 sequence and packaged in the vshRNA vector (pGCSIL-GFP). The resulting novel RNAi lentivirus vector was named as M19-pGCSIL. M19-pGCSIL was amplified and the final titer was  $1 \times 10^{10}$ /ml. H1299 cells, a lung adenocarcinoma cell line that expresses MED 19, was used. This cell line was cultured in 1640 medium mixed with 10% fetal bovine serum. The cells were divided into different groups according to the transfected vectors: Group C was transfected with empty H1299, Group N was transfected with the negative control lentivirus (PSC-NC), and Group K was transfected with M19-pGCSIL. The knockdown efficiency was measured using quantitative PCR (qPCR). The upstream primer was TGA CAG GCA GCA CGA ATC and the downstream primer was CAG GTC AGG CAG GAA GTT AC. Total RNA was extracted from the cells according to instruction. The SYBR Master Mixture kit was used for the qPCR analysis. The following were added to the reaction: 10 µl SYBR premix ex Taq, 5 µM concentrations of upstream and downstream primers, 1 µl cDNA, and 8.0 µl ddH<sub>2</sub>O (total volume of 20 µl). The following two-step reaction conditions were used: pre-linearization at 95 °C for 15 s and 45 cycles of melting at 95 °C for 5 s, annealing, and extension at 60 °C for 30 s. Light absorption was recorded at each extension stage. The total length of the qPCR product was 107 base pairs. The numerical analysis method was  $2^{-\Delta\Delta CT}$ . Western blot analysis was carried out to detect the interference result in the inner cell probation procedure using 30 µg of protein in a 12% polyacrylamide gel for sodium dodecyl sulfate polyacrylamide gel electrophoresis.

#### Cell clone conformation and MTT tests

H1299 cells were divided into the following three groups: Group C consisted of empty cells, Group N infected with PSC-NC as the negative control, and Group K transfected with M19-pGCSIL. For cell clone conformation, the initial inoculation concentration was  $2 \times 10^3$ /ml. The cells were cultured in six-well plates and the culture fluid was changed every three days. Cell clones were counted on the 14th day. The cells were Giemsa-stained for 10 min and then imaged. For the 3-(4, 5-dimethylthiazol-2-yl)-2,5-diphenyltetrazolium bromide (MTT) assay, the initial culture concentration was 1500 cells/well. The cells were grown for six days in 96-well plates before testing.

#### Propidium iodide fluorescence-activated cell sorting

As previously described, H1299 cells were separated into three groups. The cells were cultured in six-well

**Table 3. qPCR Results**

Sample	Actin Ct ( $\bar{x}\pm SD$ )	Subject Ct ( $\bar{x}\pm SD$ )	$\Delta Ct$ ( $\bar{x}\pm SD$ )	$-\Delta\Delta Ct$ ( $\bar{x}\pm SD$ )	$2^{-\Delta\Delta Ct}$ ( $\bar{x}\pm SD$ )
C	13.100 $\pm$ 0.0300	21.207 $\pm$ 0.0710	8.107 $\pm$ 0.1007	0.156 $\pm$ 0.1007	1.116 $\pm$ 0.0782
N	13.177 $\pm$ 0.0153	21.440 $\pm$ 0.0264	8.263 $\pm$ 0.0416	-0.000 $\pm$ 0.0416	1.000 $\pm$ 0.0286
K	13.223 $\pm$ 0.0153	22.233 $\pm$ 0.0306	9.010 $\pm$ 0.0458	-0.747 $\pm$ 0.0458	0.596 $\pm$ 0.0189

**Table 4. MTT Testing of Effect of M19-pGCSIL Transfection on H1299 Cell Growth**

	1 d ( $\bar{x}\pm SD$ )	2 d ( $\bar{x}\pm SD$ )	3 d ( $\bar{x}\pm SD$ )	4 d ( $\bar{x}\pm SD$ )	5 d ( $\bar{x}\pm SD$ )	6 d ( $\bar{x}\pm SD$ )
C	0.132 $\pm$ 0.0015	0.178 $\pm$ 0.0011	0.455 $\pm$ 0.0040	0.593 $\pm$ 0.0111	1.146 $\pm$ 0.0127	1.400 $\pm$ 0.0147
N	0.113 $\pm$ 0.0015	0.210 $\pm$ 0.0057	0.388 $\pm$ 0.0023	0.612 $\pm$ 0.0040	1.023 $\pm$ 0.0165	1.302 $\pm$ 0.0161
K	0.100 $\pm$ 0.0015	0.116 $\pm$ 0.0044	0.181 $\pm$ 0.0011	0.255 $\pm$ 0.0030	0.331 $\pm$ 0.0196	0.479 $\pm$ 0.0061

plates. Three control plates were set up in each group. When the cells reached 95% confluence, they were collected and centrifuged for 5 min at 1200 rpm and 4 °C. The cell pellets were washed twice with phosphate-buffered saline (PBS) (pH = 7.2–7.4) and then fixed in 70% ethanol at 4 °C. The cells were centrifuged at 1200 rpm for 5 min to remove the ethanol, suspended in PBS, and filtered through a steel sieve (400 mesh). The PBS was then removed by centrifugation and 1 ml propidium iodide was added to determine the cell cycle stage distribution by flow cytometry.

#### Transwell test

H1299 cells, which were divided into three groups as described above, were used for the Transwell experiment using a Cell Invasion Assay Kit according to the manufacturer's instructions. In 24-well plates, each upper chamber was filled with 300  $\mu$ l of serum-free culture medium and the lower chamber was filled with 500  $\mu$ l of culture medium with fetal bovine serum. The cells were cultured for 72 h. Non-invasive cells were removed with a cotton pledget and the upper chamber was dipped in 500  $\mu$ l of liquid dye for 20 min to stain the invasive cells on the inside surface of the membrane. The changer was then washed three times and air-dried. Images of the membranes were captured under a microscope. The membranes were then dissolved in 10% acetic acid for the OD 570 test.

## Results

An effective interference site on the MED 19 gene that could silence MED 19 protein expression by viral vector plasmid was screened. Four sites marked K1–K4 were chosen, among which K3 performed well. The fluorescence images showed good transfection and interference efficiencies for K3. The resulting sequence was 5'-CGA ATC TGA TCA CAC ACT A-3'.

Subsequently, the efficiency was tested using western blot analysis (Figure 1). GAPDH was chosen as the housekeeping protein for the loading control, whereas the primary antibody was mouse anti-GAPDH (1:5000). Group C did not show any labeling. Hence, no FLAG was detectable in the cells. Conspicuously, Group K3 was the weakest in both dosages of interference vectors (0.25 or 0.5  $\mu$ g). This indicates that the FLAG tail was knocked down, which indirectly shows that K3 satisfactorily silences MED 19 expression. To verify this screening result, qPCR was performed (Table 1 and Figure 2).

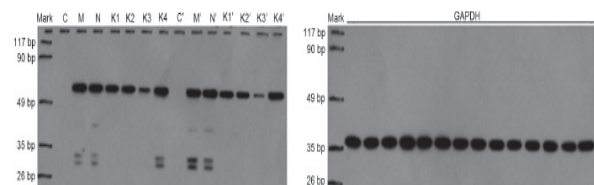


**Figure 1. Western Blot Analysis.** Left, C: Non-transfected 293T cells as negative control; M: Transfected with 0.5  $\mu$ g pEGFP-N1-3FLAG; N: Transfected with 0.5  $\mu$ g empty viral vector plasmid; K1-K4: Transfected with 0.5  $\mu$ g of various viral vector plasmids targeting MED 19 sequences: C', M', N', K'1–K'4 were transfected with 0.25  $\mu$ g of interference vector. Group C was negative control, K1-K4 were different targets on MED 19. K3 was the weakest in both dosages of interference vectors, which showed a perfect knocking down efficiency of FLAG tail, indirectly inferred that K3 could silence MED 19 expression satisfactorily. Right: House-keeping gene GAPDH. GAPDH as the housekeeping protein was chosen to be loading control

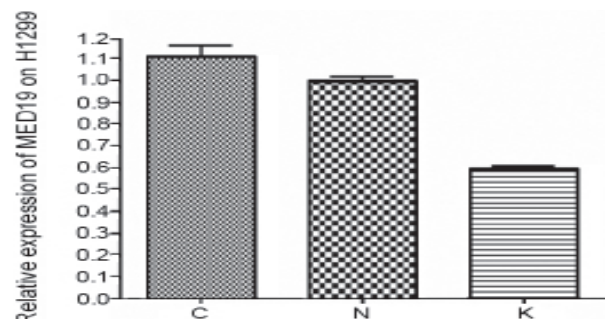


**Figure 2. Relative Expression of MED 19.** In order to verify the screening result above, H1299 cell line expresses MED 19 was utilized. Group N consist of H1299 cells transfected with empty lentivirus (PSC-NC, control construct), Group C was non-transfected, and Group K was transfected with M19-pGCSIL. Results were tested by qPCR and the value of  $2^{-\Delta\Delta Ct}$  reflects the relative expression of each sample compared with Group N. Group K is much lower than C and N ( $p < 0.05$ , paired sample test), it knocked down MED 19 significantly by 55%

As described in Table 3, Group N consisted of H1299 cells transfected with empty lentivirus (PSC-NC, control construct), Group C was non-transfected, and Group K was transfected with M19-pGCSIL. In the qPCR analysis, the value of  $2^{-\Delta\Delta Ct}$  reflects the relative expression of each sample compared with Group N (Figure 2). Group K expressed less MED 19 mRNA at slightly more than half than those with Group N. Therefore, M19-pGCSIL was able to knock down MED 19 ( $p < 0.05$ , paired sample test) more efficiently than Group N. The knockdown efficiency of Group K was 55%.



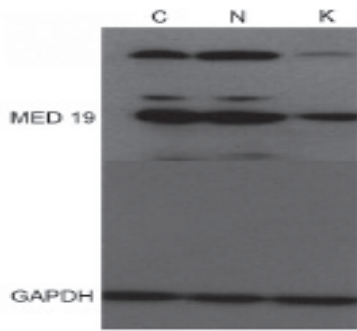


**Figure 3. Western Blot to Test the Endogenous Levels of M19-pGCSIL Knock-down Efficiency.** Testing of the endogenous levels of M19-pGCSIL knock-down efficiency in H1299 cells was performed by western blot as shown here. Group C was normal untransfected H1299, Group N was H1299 transfected with negative control lentivirus (PSC-NC) and Group K was transfected with M19-pGCSIL, GAPDH as the housekeeping protein was chosen to be loading control. Lane C showed MED 19 was highly expressed. There was no silencing effect in Lane N. Lane K was H1299 transfected with M19-pGCSIL, an RNAi lentivirus aimed at MED 19. The band for Lane K was narrow and weak compared to Lane C; MED 19 quantity was much lower

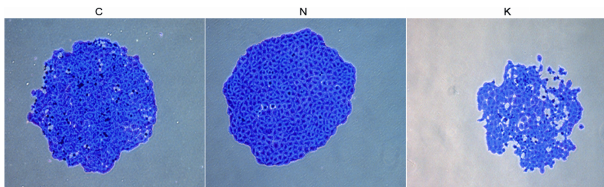


**Figure 4. Cell Colony Conformation Test Results.** C: Empty H1299 cells stained by Giemsa; N: H1299 cells infected with PSC-NC (empty control lentivirus), stained by Giemsa; K: H1299 cell transfected with M19- pGCSIL, stained by Giemsa; It could be seen clearly cell count in K was much lower than that in C and N. We consider it to be the result of M19- pGCSIL transfection, which suppressed MED 19 expression leading to a significant impairment of colony conformation

To test the knockdown efficiency of M19-pGCSIL, the H1299 cell line was utilized and MED 19 was assessed by western blot (Figure 3). RNAi lentivirus M19-pGCSIL was transfected into H1299, a lung adenocarcinoma cell line that normally expresses MED 19. The western blot band for the infected H1299 cells was narrow and weak compared with that of normal cells. Hence, the quantity of MED 19 was much lower. M19-pGCSIL was confirmed as an interfering lentivirus that can knock down MED 19 expression. Subsequently, how the biological behaviors of H1299 cells are changed after silencing was determined. After transfecting M19-pGCSIL into the H1299 cells, MED 19 expression was suppressed. The cells were weak during colony formation (Figure 4). The cluster of H1299 cells infected with M19-pGCSIL was thin and sparse. The clone count in Group K was much lower than in Groups C and D (Figure 4). The difference was considered a result of MED 19 silencing. Upon infection with M19-pGCSIL, the ability of infected H1299 cells to form a cell colony was weaker than the ability of normal H1299 cells.

In the MTT assay, live cells were stained by thiazolyl blue. The staining intensity was tested using a spectrophotometer at OD 570, which indirectly showed the number of living cells and growth velocity (Table 4

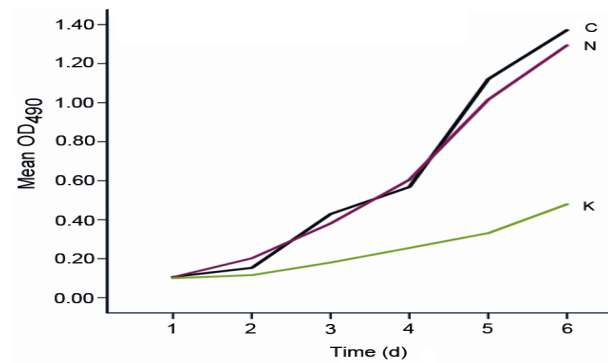


**Figure 5. MTT Test Curve.** In MTT test, live H1299 cells were stained by thiazolyl blue and tested. The values of OD 570 forms Y-axis, X-axis is time (d). The graph showed the number of living cells and growth velocity indirectly. C was empty H1299 cells, N was H1299 cells infected with PSC-NC (empty control lentivirus), K was H1299 cell transfected with M19- pGCSIL. Live cells in the three groups increased as time went on, but curve slope values of C and N were higher than K, so cells grew faster than K and live cells were more. On the other hand, cells in K were less and grew slower (SPSS V13.0, One-way ANOVA,  $p < 0.05$ )

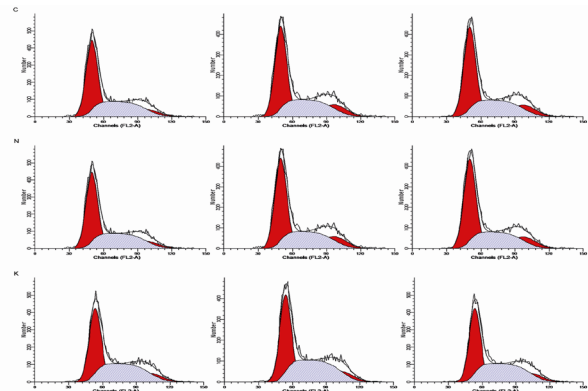


**Figure 6. Flow Cytometry for Cell Cycle Analysis.** The cell cycle is divided into four phases: G1, S, G2 and M. G1: Growth and preparation of the chromosomes for replication; S: Synthesis of DNA and duplication of the centrosome; G2: Preparation for mitosis; M: Mitosis. In this figure, Y-axis is cell number, X-axis is channel (It can distinguish different cell cycle phases). The first peak was G1, it was sharp, high and narrow. The second peak was S, it was dull, low and wide. The third one was G2/M. C was empty H1299 cells, N was H1299 cells infected with PSC-NC (empty control lentivirus), K was H1299 cell transfected with M19- pGCSIL. Compared with C and N, for K, the number of cells in S-phase of the cell cycle increased, meanwhile, the number decreased in both G1 and G2/M. It seemed that Group K was blocked in S phase and inhibited from entering G2/M

and Figure 5) (Wilson, 2000; Bernas and Dobrucki, 2002). The data were used to analyze the difference between the treatment groups. The graphs shown in Figure 5 present the increase in the number of living cells with time. The living cell number in Group K (H1299 cells transfected with M19-pGCSIL) increased more slowly than the other groups. The slow growth indicates fewer living cells in Group K compared with Groups C and N. Transfection with the MED 19 knockdown lentivirus slowed the growth of the H1299 cells. (SPSS V13.0, one-way ANOVA,  $p < 0.05$ ).

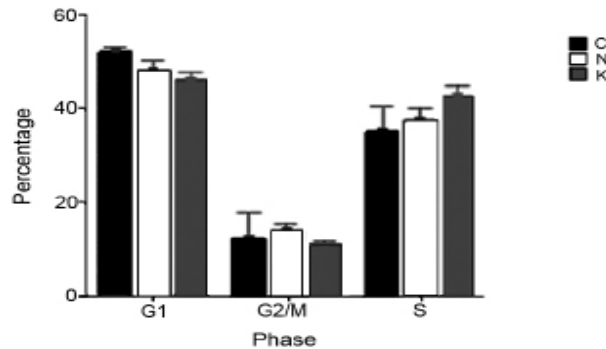
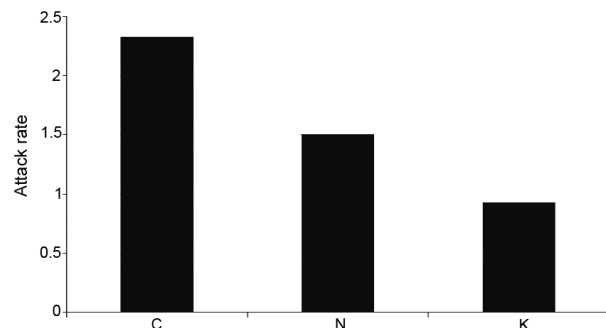
Flow cytometry detected an increase in the number

**Table 5. Cell Cycle Test Classification**

	G1 ( $\bar{x} \pm SD$ )	G2/M ( $\bar{x} \pm SD$ )	S ( $\bar{x} \pm SD$ )
C	52.353±0.3754	12.410±2.2783	35.240±2.1039
N	48.330±0.8240	13.990±0.5923	37.677±1.0355
K	46.253±0.6901	11.017±0.1804	42.733±0.8591

**Table 6. MTT Value of Transwell Test**

	MTT value (when cultured, $\bar{x} \pm SD$ )	OD value (after dyeing, $\bar{x} \pm SD$ )	Attack rate
C	0.249±0.0056	0.578±0.0009	2.327
N	0.244±0.0054	0.366±0.0012	1.497
K	0.188±0.0019	0.174±0.0009	0.926

**Figure 7. Cell Cycle Distribution as Determined by Flow Cytometry.** In this graph, Y-axis shows the proportion of different cell cycle phases, X-axis is cell cycle phases, C was empty H1299 cells, N was H1299 cells infected with PSC-NC (empty control lentivirus), K was H1299 cell transfected with M19-pGCSIL. It showed an increase in the number of cells in S-phase of the cell cycle and a decrease in G1, G2/M cell numbers for K**Figure 8. Attack Rate of Different Groups.** In transwell migration assays, a series of MTT values were obtained. Y-axis is attack rate calculated from MTT values (numbers were analyzed in SPSS v13.0, expressed as  $\bar{x} \pm SD$ , Attack rate = MTT value/OD value), X-axis is the different cells. C was empty H1299 cells, N was H1299 cells infected with PSC-NC (empty control lentivirus), K was H1299 cell transfected with M19-pGCSIL. We can see that the attack rate of Group K was lower than the other two groups (SPSS v13.0,  $p < 0.05$ )

of cells in the S phase of the cell cycle and a decrease in G1 and G2/M cell numbers (Table 5, Figure 6 and 7). According to the graph (Figures 6 and 7), G1 and G2/M exhibited a decrease in the number of cells whereas the number of cells in the S phase increased when the H1299 cells were transfected with M19-pGCSIL. DNA replicates during the S phase, thus, the DNA content is doubled. Group K cells were apparently blocked during the S phase and were inhibited from entering G2/M. As a result, the cells in Group K were not affected by the

DNA replication after transfection. However, mitosis was affected. Therefore, cell number was lower in Group K than in Groups C and N. This confirms the results observed in the cell clone conformation test (Figure 6).

The metastatic ability was weaker as demonstrated by the Transwell migration assays (Table 6 and Figure 8). Initially, three cell groups (C, N, and K) were cultured. The MTT value of each group was tested. The cells were cultured for 72 h and tested again (analyzed in SPSS v13.0, expressed as  $\bar{x} \pm SD$ , attack rate = MTT value/OD value). The attack rate of Group K was lower than those of the other two groups (SPSS v13.0,  $p < 0.05$ ). The cells expressing less MED 19 displayed weaker metastatic abilities (Figure 8).

## Discussion

This study investigated the function and possible pathway of MED 19 silencing in the non-small cell lung carcinoma cell line (H1299). Four principal findings were obtained: 1) cells in the MED 19-silenced group had a weak clone colony formation ability, 2) cell growth velocity was lower in the MED 19-silenced group, 3) cells were inclined to be arrested in the S phase of the cell cycle and had trouble advancing from the S phase to the M phase (mitosis), and 4) the MED 19-silenced cells displayed a weak invasive capability.

In the past, lung carcinoma therapies have proven very ineffective. Inhibiting and removing the primary lesion was sometimes insufficient and carcinoma cells often metastasized to remote tissues and caused recurrent carcinomas or other serious complications (Long et al., 2010). Inhibiting metastasis may be a promising method for controlling carcinoma (Ramaswamy et al., 2003). The first step in carcinoma cell metastasis is invasion through the basement membrane of a blood vessel (Yoshida et al., 2000; Chiang and Massague, 2008; Klein, 2008). During this process, matrix-degrading enzymes play important roles. In the present experiment, a newly identified protein called MED 19 was utilized. MED 19 is a co-activator that is required for the activation of RNA polymerase II transcription by DNA-bound transcription factors. MED is a multiprotein coactivator that promotes RNA polymerase II transcriptional activation through direct interaction with transcription factors bound to enhancers and upstream promoter elements and with polymerase and the general initiation factors at the core promoter (Myers and Kornberg, 2000; Mittler et al., 2001). MED 19 is a subunit of MED and it plays a critical role in the activation and repression of mRNA synthesis in eukaryotic cells. In humans, MED 19 is also known as LCMR1. The basal activation and transcription efficiency of MED reaches only 30% of wild-type levels when MED 19 is removed from MED. RNAi is a widely used method for silencing or decreasing protein expression. In the current experiment, different segments of the Med 19 gene were targeted using RNAi. Targeting a sequence in the second exon of the MED 19 open reading frame (242–261 in CDS) led to the efficient knockdown of MED 19. The interference efficiency was satisfactory. Consequently, a new RNAi lentivirus called M19-pGCSIL was constructed, which

was transfected into H1299 cells and the biological behavior of H1299 cells was tested.

The MED 19 encoded protein is called LCMR1; in vitro experiments showed that MED 19 participates in cell cycle regulation, signal transduction, and transcriptional control by changing its location and motion in cells (Sato et al., 2004; Ding et al 2009). The NF- $\kappa$ B family of transcription factors is crucial for the expression of multiple genes involved in cell survival, proliferation, differentiation, and inflammation. The expression of many endogenous NF- $\kappa$ B target genes depends on the interaction between p65 and MED, which occurs through the Trap-80 subunit of MED and the TA1 and TA2 regions of p65. The Drosophila NF- $\kappa$ B homologue Dif has been shown to interact with MED 17. Although no obvious human sequence homology with Dif has been found, Dif is assumed to correspond to the mammalian MED subunit Trap-80 (Orphanides et al., 1996; Hoffmann and Baltimore, 2006).

In *Saccharomyces cerevisiae*, kin28 is a cyclin-dependent kinase. It is a subunit of the basal transcription factor holo-TFIID and its trimeric subcomplex TFIID. kin28 phosphorylates the C-terminal domain (CTD) of RNA polymerase II (RNA pol II) within a transcription initiation complex. MED enhances the phosphorylation of the CTD of RNA pol II by holo-TFIID in vitro. The TFIID subunits are sufficient for MED to enhance kin28 CTD kinase activity and the phosphorylation of a glutathione S-transferase-CTD fusion protein. MED does not stimulate the activity of several other CTD kinases, which suggests that the specific enhancement of TFIID kinase activity results in kin28 as the primary CTD kinase at initiation (Guidi et al., 2004; Tokusumi et al., 2007).

The mechanism by which MED 19 takes part in cell cycle regulation and altering invasiveness remains undetermined. A decrease in MED 19 in speculated cause stagnation in the S phase in vitro, which is strongly indicated by the present experimental results. DNA is synthesized and the centrosome is duplicated during the S phase in preparation for mitosis. If cells are arrested in the S phase, fewer cells enter the G2 and M phases, resulting in a lower total number of cells. The Transwell experiments show that decreased MED 19 expression causes cells to have decreased invasiveness or metastatic capacity. The possible functional sites of other MEDs, including NF- $\kappa$ B, kin28 in holo-TFIID, and TFIID, in almost all other species except humans were reviewed. The next step in this research is the identification of human sequences that are homologous to these sequences in other species and determining the mechanism by which MED 19 affects cell division and migration.

## References

- Baidoobonso SM, Guidi BW, Myers LC (2007). Med19 (Rox3) regulates intermodule interactions in the *Saccharomyces cerevisiae* mediator complex. *J Biol Chem*, **282**, 5551-9.
- Bernas T, Dobrucki J (2002). Mitochondrial and nonmitochondrial reduction of MTT: interaction of MTT with TMRE, JC-1, and NAO mitochondrial fluorescent probes. *Cytometry*, **47**, 236-42.
- Bjorklund S, Gustafsson CM (2005). The yeast Mediator complex and its regulation. *Trends Biochem Sci*, **30**, 240-4.
- Boyer TG, Martin ME, Lees E, Ricciardi RP, Berk AJ (1999). Mammalian Srb/Mediator complex is targeted by adenovirus E1A protein. *Nature*, **399**, 276-9.
- Chiang AC, Massague J (2008). Molecular basis of metastasis. *N Engl J Med*, **359**, 2814-23.
- Conaway RC, Sato S, Tomomori-Sato C, Yao T, Conaway JW (2005). The mammalian Mediator complex and its role in transcriptional regulation. *Trends Biochem Sci*, **30**, 250-5.
- Ding N, Tomomori-Sato C, Sato S, et al (2009). MED19 and MED26 are synergistic functional targets of the RE1 silencing transcription factor in epigenetic silencing of neuronal gene expression. *J Biol Chem*, **284**, 2648-56.
- Guidi BW, Bjornsdottir G, Hopkins DC, et al (2004) Mutual targeting of mediator and the TFIID kinase Kin28. *J Biol Chem*, **279**, 29114-20.
- Gu W, Malik S, Ito M, et al (1999). A novel human SRB/MED-containing cofactor complex, SMCC, involved in transcription regulation. *Mol Cell*, **3**, 97-108.
- Hoffmann A, Baltimore D (2006). Circuitry of nuclear factor kappaB signaling. *Immunol Rev*, **210**, 171-86.
- Kim YJ, Bjorklund S, Li Y, Sayre MH, Kornberg RD (1994). A multiprotein mediator of transcriptional activation and its interaction with the C-terminal repeat domain of RNA polymerase II. *Cell*, **77**, 599-608.
- Klein CA (2008). Cancer. The metastasis cascade. *Science*, **321**, 1785-7.
- Long N, Moore MA, Chen W, et al (2010). Cancer epidemiology and control in north-East Asia - past, present and future. *Asian Pac J Cancer Prev*, **Suppl 2**, 107-48.
- Mittler G, Kremmer E, Timmers HT, Meisterernst M (2001). Novel critical role of a human Mediator complex for basal RNA polymerase II transcription. *EMBO Rep*, **2**, 808-13
- Myers LC, Kornberg RD (2000). Mediator of transcriptional regulation. *Annu Rev Biochem*, **69**, 729-49.
- Orphanides G, Lagrange T, Reinberg D (1996). The general transcription factors of RNA polymerase II. *Genes Dev*, **10**, 2657-83.
- Ramaswamy S, Ross KN, Lander ES, Golub TR (2003). A molecular signature of metastasis in primary solid tumors. *Nat Genet*, **33**, 49-54.
- Sato S, Tomomori-Sato C, Banks CA, et al (2003). Identification of mammalian Mediator subunits with similarities to yeast Mediator subunits Srb5, Srb6, Med11, and Rox3. *J Biol Chem*, **278**, 15123-7.
- Sato S, Tomomori-Sato C, Parmely TJ, et al (2004). A set of consensus mammalian mediator subunits identified by multidimensional protein identification technology. *Mol Cell*, **14**, 685-91.
- Tokusumi Y, Ma Y, Song X, Jacobson RH, Takada S (2007). The new core promoter element XCPE1 (X Core Promoter Element 1) directs activator-, mediator-, and TATA-binding protein-dependent but TFIID-independent RNA polymerase II transcription from TATA-less promoters. *Mol Cell Biol*, **27**, 1844-58.
- Wang W, Zhang N, Wang J, Bu XM, Zhao CH (2011). Inhibition of proliferation, viability, migration and invasion of gastric cancer cells by Aurora-A deletion. *Asian Pac J Cancer Prev*, **12**, 2717-20.
- Wilson AP (2000). Cytotoxicity and Viability Assays in Animal Cell Culture: A Practical Approach. *Oxford University Press: Oxford*.
- Yoshida BA, Sokoloff MM, Welch DR, Rinker-Schaeffer CW (2000). Metastasis-suppressor genes: a review and perspective on an emerging field. *J Natl Cancer Inst*, **92**, 1717-30.